JOURNAL OF APPLIED ELECTROCHEMISTRY 23 (1993) 1139–1146

Effect of gas evolution on mass transfer in an electrochemical reactor

W. S. WU, G. P. RANGAIAH

Department of Chemical Engineering, National University of Singapore, Singapore 0511, Republic of Singapore

Received 17 August 1992; revised 8 February 1993

Experiments were conducted to study the effect of gas bubbles generated at platinum microelectrodes, on mass transfer at a series of copper strip segmented electrodes strategically located on both sides of microelectrodes in a vertical parallel-plate reactor. Mass transfer was measured in the absence and presence of gas bubbles, without and with superimposed liquid flow. Mass transfer results were compared, wherever possible, with available correlations for similar conditions, and found to be in good agreement. Mass transfer was observed to depend on whether one or all copper strip electrodes were switched on, due to dissipation of the concentration boundary layer in the interelectrode gaps. Experimental data show that mass transfer was significantly enhanced in the vicinity of gas generating microelectrodes, when there was forced flow of electrolyte. The increase in mass transfer coefficient was as much as fivefold. Since similar enhancement did not occur with quiescent liquid, the enhanced mass transfer was probably caused by a complex interplay of gas bubbles and forced flow.

List of symbols

A	electrode area (cm^2)
a	constant in the correlation ($k = aRe^m$, $cm\,s^{-1}$)
$C_{R,bulk}$	concentration of the reactant in the bulk ($mol^{-1}\,dm^{-3}$)
D	diffusion coefficient ($cm^2\,s^{-1}$)
d_h	hydraulic diameter of the reactor (cm)
F	Faraday constant
Gr	Grashof number = $gL^3\Delta\rho/\nu^2\bar{\rho}$ (dimensionless)
g	gravitational acceleration ($cm\,s^{-2}$)
i_g	gas current density ($A\,cm^{-2}$)
i_L	mass transfer limiting current density ($A\,cm^{-2}$)
k	mass transfer coefficient ($cm\,s^{-1}$)
L	characteristic length (cm)
m	exponent in correlations
n	number of electrons involved in overall electrode reaction, dimensionless
Re	Reynolds number = $Ud_h\nu^{-1}$ (dimensionless)
Sc	Schmidt number = νD^{-1} (dimensionless)
Sh	Sherwood number = kLD^{-1} (dimensionless)
U	mean bulk velocity ($cm\,s^{-1}$)
x	distance (cm)
δ_N	'equivalent' Nernst diffusion layer thickness (cm)
ν	kinematic viscosity ($cm^2\,s^{-1}$)
$\Delta\rho$	density difference = $(\rho_L - \bar{\rho})$, ($g\,cm^{-3}$)
ρ_L	density of the liquid ($g\,cm^{-3}$)
$\bar{\rho}$	average density of the two-phase mixture ($g\,cm^{-3}$)
ϵ	void fraction (volumetric gas flow/gas and liquid flow)

1. Introduction

Gas evolution in electrochemical reactors occurs widely in the electrochemical industry. The presence of gas bubbles in an electrochemical reactor affects both dispersion or mixing [1,2] and mass transfer [3] of ionic species within the reactor. Effect of gas bubbles on mass transfer in electrochemical reactors was studied in three different situations: (i) mass transfer at gas evolving electrodes; (ii) mass transfer at working electrodes in the presence of gas sparging to create bubbles and (iii) mass transfer to working electrodes in the presence of gas generating electrodes. These studies were conducted with and/or without superimposed electrolyte flow. Another situation studied was mass transfer enhancement due to gas bubbles produced at the counter electrode [e.g. 4 and 5]. This may be considered as a special case of the third situation above.

Mass transfer at vertical gas evolving electrodes has been widely investigated [e.g. 6–9]; references [10] and [11] report mass transfer at horizontal electrodes. Recently, mass transfer at the gas evolving inner electrode of a concentric cylindrical reactor was reported in [12]. A number of models have been proposed for mass transfer at gas evolving electrodes. A good summary and discussion of these models is presented in [13]. Ibl [14], Sigrist *et al.* [15], Cavatorta *et al.* [16] among others, have reported mass transfer studies in the presence of gas sparging. However,

0021-891X

only limited results are available in the literature concerning mass transfer enhancement due to gas generating electrodes strategically situated close to the working electrodes where the mass transfer is being measured [7,17]. Such strategic placement allows the investigation of the effect of gas bubbles on the concentration boundary layer near gas generating electrodes.

This paper presents experimental findings on mass transfer enhancement due to gas evolution at microelectrodes flush mounted on the wall of a vertical parallel-plate electrochemical reactor, under a range of operating conditions. Spacing and sizing of working electrodes were such that localized mass transfer coefficients were obtained at different distances on both sides of gas-generating microelectrodes, and the effect of gas bubbles on the concentration boundary layer was ascertained.

2. Experimental details

2.1. *Mass transfer measurement*

The measurement of mass transfer enhanced by the presence of bubbles was determined by using the limiting diffusion current technique [18]. A well defined limiting-current plateau must be detected in the current–potential plot in order to justify the use of this method. The mass transfer coefficient of the reactant species may be obtained by assuming the reactant concentration at the electrode is zero. The mass transfer coefficient (k) is thus

$$k = \frac{i_L}{nFAC_{R,\text{bulk}}} \tag{1a}$$

If the concentration gradient throughout the diffusion layer is assumed to be linear then k can be formally related to diffusion coefficient, D and thickness of the diffusion layer, δ_N (the Nernst diffusion layer). Hence,

$$k = D/\delta_N \tag{1b}$$

The monitored reaction was copper deposition on a copper cathode at room temperature (20 °C).

2.2. *Cell design and electrolyte flow system*

The cell employed in this work was similar in dimensions and construction to that reported earlier [2]. It consisted of three Perspex sheets, two outer slabs (1.0 cm thick) separated by a thin (0.2 cm thick) spacer which defined the channel shape. A diffuser section (18 cm long, 8° half angle) was created before the parallel section to ensure fully developed flow in the cell for Reynolds' numbers up to 6000. The width to gap ratio of the channel was 25, sufficient for the flow to be considered as one dimensional.

The arrangement of electrodes for mass transfer studies was different from that reported earlier [2], and is depicted in Fig. 1. Working electrodes were copper strip cathodes of height 1 mm, flush-mounted on the wall. The vertical distance between two consecutive working electrodes was 3 mm thus providing an electrode-free gap of 2 mm. This small gap ensures high spatial resolution of mass transfer measurements both upstream and downstream of the gas-generating microelectrodes. On the anodic side of the reactor, relatively long copper plates facing the opposite copper strip cathodes, were used.

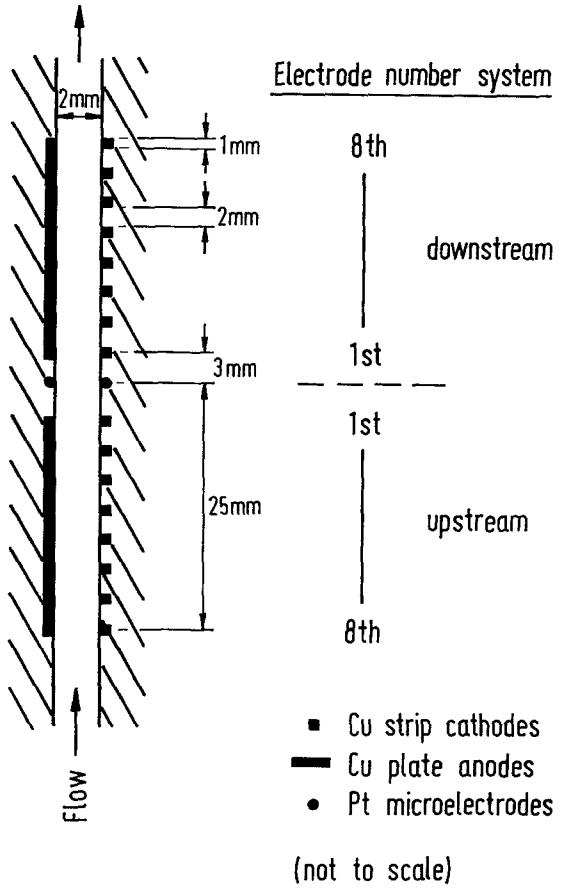

Fig. 1. Sectional view of the vertical parallel-plate electrochemical reactor.

Ten platinum wire microelectrodes of diameter 0.45 mm were used for gas generation. The horizontal distance between two platinum electrodes was 5 mm. Use of these separated platinum wire electrodes resulted in less coalescence of bubbles during gas evolution and an even curtain of gas bubbles as compared to that obtained with a strip electrode or by gas sparging. The arrangement of platinum microelectrodes at the opposite side of the channel was identical (i.e. 10 microelectrodes). Since gas generation was at electrodes flush-mounted on the wall, gas bubbles were mainly close to the wall, and not in the middle section of the channel under the flow conditions studied.

The flow arrangement was again similar to that used in the previous study [2]. The electrolyte in this case was 0.1 M Na_2SO_4 + 0.02 M H_2SO_4 + 0.01 M $CuSO_4$ + 0.02 M ethanol + 1000 p.p.m. ethylene glycol. This electrolyte has a pH of 2. The addition of small amounts of ethanol hinders the coalescence of bubbles and also provides bubbles of uniform diameter [19], while the presence of ethylene glycol reduces the adhesion forces between bubbles and the perspex wall [20].

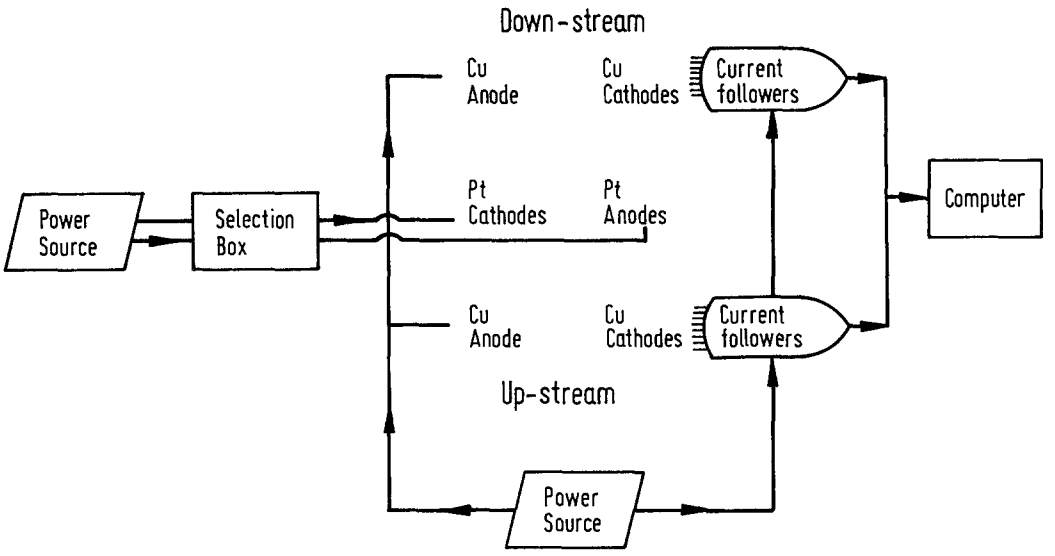

Fig. 2. Schematic instrumental diagram.

2.3. *Instrumentation and data acquisition*

Figure 2 depicts the instrumental setup for mass transfer studies. Two sets of current followers were used, one set for the upstream and another for the downstream detector electrodes. Although the cell construction shown in Fig. 1 contained eight upstream and eight downstream electrodes (with respect to the position of gas generating electrodes) only the eight downstream and six upstream positions could be monitored as only fourteen current followers were available.

The analog outputs of the current followers were fed to the computer for statistical analysis of the currents drawn at the copper electrodes (i.e. mean and standard deviation). This procedure was necessary due to fluctuation of the current caused by the presence of bubbles. Another power source with the electrode selection box was used for the generation of hydrogen and oxygen bubbles on the microelectrodes. Constant current was employed for the generation of gas. Oxygen gas was generated on the microelectrodes which were situated on the same wall as the working electrodes.

3. Results and discussion

3.1. *Mass transfer in the absence of gas*

Initially, experiments were conducted to find mass transfer coefficients in the absence of gas, with either one or all working electrodes on. Different electrolyte flow rates were employed; Reynolds numbers, Re (based on hydraulic diameter), studied were 0, 20, 70 and 120. The mass transfer coefficient, k, at a single working electrode for $Re = 20$, 70 and 120, was subsequently correlated with Re. Table 1 tabulates the gradient (m) and the coefficient (a) for the correlation, $k = aRe^m$.

When only one electrode is in operation, m and a are not expected to depend on electrode position and number. Accordingly, the results in Table 1 indicate that m and a vary over a narrow range. The average value of m is 0.353 which agrees well with 1/3 in the following correlation for mass transfer on a finite width electrode in fully developed flow conditions [21].

$$Sh = \frac{kd_h}{D}\alpha\left(ReSc\frac{d_h}{x}\right)^{1/3} \tag{2}$$

Variation in a, which is directly related to variation in k from one electrode to another at identical conditions, is more than that in m. This may be due to unavoidable differences in factors such as size, cleanliness and flush-mounting of the working electrodes in the experimental setup.

Experiments were also conducted to measure k at each electrode when all electrodes were on at $Re = 0$, 20, 70 and 120. The calculated k at each

Table 1. Results of correlation of k at single working electrode with Re in the absence of gas bubbles

Electrode position and number (d – downstream u – upstream)	*m and a in* $k = aRe^m$	
	m	$a \times 10^4$
d8	0.352	6.90
d7	0.334	6.44
d6	0.334	5.60
d5	0.332	5.79
d4	0.348	6.03
d3	0.371	5.91
d2	0.370	5.14
d1	0.373	4.32
u1	0.342	5.49
u2	0.338	5.94
u3	0.342	6.05
u4	0.362	5.91
u5	0.355	5.79
u6	0.382	5.32
Average	0.353	5.76
standard deviation	0.017	0.60

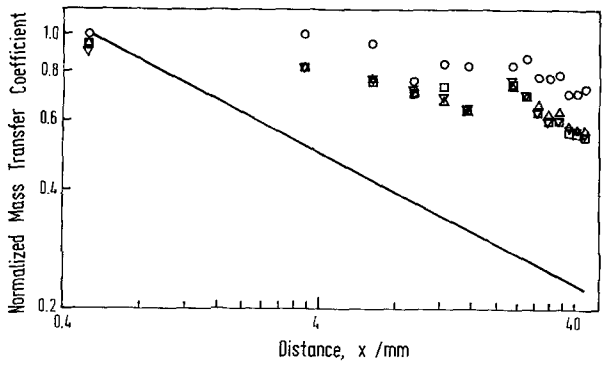

Fig. 3. Variation of normalized mass transfer coefficient with distance, in the absence of gas bubbles and all electrodes on mode. (——) k against $x^{-1/3}$ (Eqn. 2). *Re*: (○) 0, (△) 20, (□) 70 and (▽) 120.

electrode from these experimental data, was normalized with respect to the corresponding k when only that electrode was on. This is to reduce the effect of experimental error due to differences in working electrodes mentioned above.

Hence, the results are plotted in Fig. 3, in terms of normalized mass transfer coefficient, (k_{all}/k_{one}) against distance (x) from the lower edge of the upstream electrode number 6. The ratio of k_{all} to k_{one} is less than unity implying reduction of k when all electrodes are on compared to a single electrode. This is due to the progressive depletion of the reactive component and consequent building up of the concentration boundary layer near working electrodes during the 'all electrodes on' operation.

The relationship between k and x, as given by Equation 2, is not applicable because of interelectrode gaps (see Fig. 1). However, for comparison, k against $x^{1/3}$ is also shown in Fig. 3. Clearly, the present results do not follow this relationship, except possibly for downstream electrodes. Rather Fig. 3 indicates two main differences compared with Equation 2. First, k decreases slowly with x particularly for upstream electrodes. Second, there is a sudden change in k going from upstream electrodes to downstream electrodes.

The observed differences may be due to the arrangement of the working electrodes: copper strip cathodes of 1 mm height positioned with a clear gap of 2 mm between two consecutive cathodes (see Fig. 1). Also, there is a clear gap of 6 mm between the upstream and downstream set of electrodes. This permits relaxation or reduction of the concentration boundary layer (whose thickness is estimated to be in the order of 100 μm for the present experimental conditions), resulting in a k weakly dependent on x, particularly for upstream electrodes.

Figure 3 shows that there is a clear difference between the data for $Re = 0$ and those in the presence of forced convection. The decrease of k with x seems to be slower at $Re = 0$ compared to that when the liquid is flowing. The relaxation of concentration boundary layer due to interelectrode gaps is probably crucial in making k less dependent on x for the case of $Re = 0$ when the concentration boundary layer is expected to be thicker compared to that in the presence of forced convection.

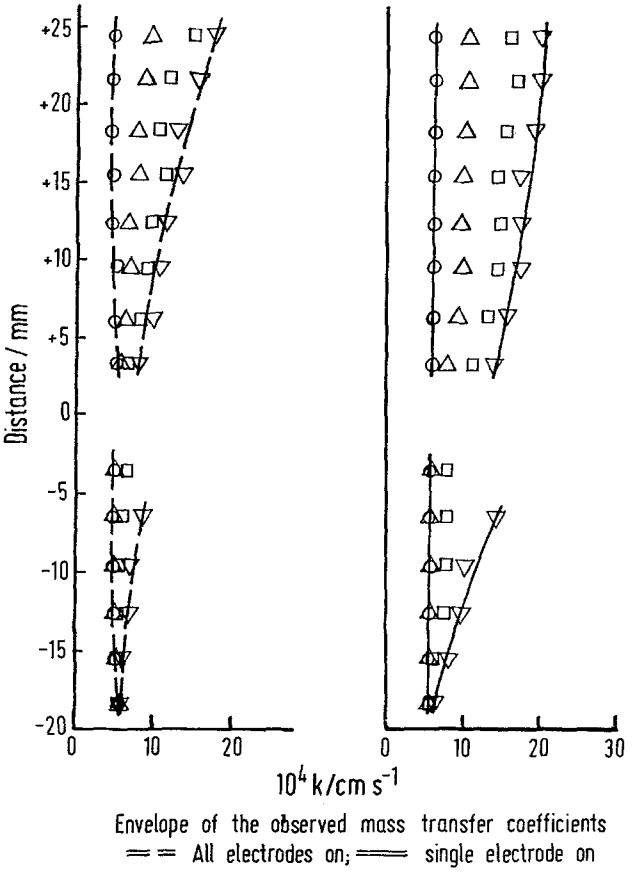

Fig. 4. Variation of mass transfer coefficient with distance from gas generating sites and gas void fraction at *Re*: 0. i_g: (○) 0.00, (△) 1.05, (□) 3.15 and (▽) 6.28.

3.2. *Mass transfer in the presence of gas and quiescent liquid*

A series of experiments was conducted to study the effect of oxygen gas bubbles on k. Liquid flow was varied to cover *Re* from 0 to 120, and tests were done with one electrode on as well as with all electrodes on. This section describes the results for the case of quiescent liquid. Results in the presence of forced convection (i.e. $Re > 0$) are discussed in the subsequent section. The gas-producing current was varied from 0 (no gas situation) to 180 mA, which corresponds to a maximum current density of 18.9 A cm^{-2}.

Results for the simplest situation of $Re = 0$ are presented in Fig. 4 in terms of k as a function of distance from gas generation sites. Data for all electrodes on are shown on the left side while those for single electrodes are shown on the right side. Under similar conditions, k for a single electrode on is usually larger than that for the case of all electrodes on. This behaviour was similar to that noted in the earlier section for the no gas situation, and is due to the build up of the concentration boundary layer.

Figure 4 shows that the effect of gas current density, i_g on k, is somewhat different depending on the location of the electrodes, for either all or a single electrode on situation. There are three regions: upstream

Table 2. Correlation of k versus i_g^m in the presence of gas bubbles and with quiescent liquid

Downstream electrode number	*m for all electrodes on*	*m for single electrode on*
d8	0.328	0.381
d7	0.320	0.385
d6	0.302	0.372
d5	0.289	0.344
d4	0.303	0.381
d3	0.301	0.328
d2	0.298	0.304
d1	0.320	0.313

electrodes, electrodes in the vicinity of gas generation sites and downstream electrodes. It appears that i_g has a marginal effect on k at upstream electrodes when they are distant. When an upstream electrode is close to the gas generation sites, k increases with i_g, particularly when i_g is high. The limited data and the marginal effect in some cases make further analysis difficult.

It may be noted that a small increase of k at electrodes located below the gas-generating electrodes and in the absence of forced flow, was also reported in [7]. The differences in those and the present experiments are mainly the dimensions of the working electrodes used. Earlier work has employed relatively larger electrodes both for gas generation (>2 mm against 0.45 mm in this study) and for mass transfer measurements (4 mm against 1 mm). Mass transfer enhancement at working electrodes close to gas generation will be further discussed in the next section.

The effect of i_g on downstream electrodes appears to be uniform. Hence, k at each electrode was correlated with i_g^m. Values of the exponent, m, are presented in Table 2. The value of m for the case of all electrodes on appears to be smaller than that for the case of a single electrode on. The present set of experiments is analogous to those using gas sparging or the introduction of gas at the counter electrodes and with no forced convection. In the present study, electrogenerated gas bubbles were introduced at the same wall as that at which mass transfer was studied. But there is no co-evolution of gas at the working electrodes. Convection is then solely due to changes in the hydrodynamics induced by gas bubbles.

Mass transfer due to natural turbulent convection at plane walls is given by [25]:

$$Sh \propto (Gr\,Sc)^{1/3} \tag{3}$$

where

$$Gr = \frac{gL^3}{\nu^2}\left[\frac{\Delta\rho}{\bar{\rho}}\right] = \frac{gL^3}{\nu^2}\left[\frac{\epsilon}{1-\epsilon}\right] \tag{4}$$

For small values ϵ (say, $\epsilon \leq 0.1$), the ratio $\epsilon/(1-\epsilon)$ is close to ϵ. Hence, Equation 3 gives $k \propto \epsilon^{1/3}$. Assuming that ϵ is proportional to i_g, $k \propto i_g^{1/3}$. The estimated m values in Table 2 are in accord with this prediction, and also with the experimental data on gas sparging in [15].

Figure 4 further indicates that k at downstream electrodes gradually increases with distance from gas-generating microelectrodes. The extent of increase varies from negligible at zero gas current to almost double at the highest gas current studied and all electrodes on. Possible factors contributing to this phenomenon are: (i) the increase in bubble velocity and size as bubbles rise and coalesce, and the consequent effect on mixing; (ii) migration of a few bubbles from the wall region to the central region thus improving macromixing; and (iii) the effect of bubbles which tend to accumulate (and possibly recirculate) at the top when the electrolyte is stagnant.

3.3. *Mass transfer in the presence of gas and forced convection*

This section discusses experimental results on the effect of oxygen gas bubbles on k in the presence of forced convection. In these experiments, three Re numbers and five gas currents were considered. Both the scenarios – all and one electrode on – were studied. Results are presented in Figs 5, 6 and 7 for $Re = 20$, 70 and 120, respectively. To improve clarity, data for a few intermediate gas currents, although available, are not included in these figures.

The void fraction of the gas (ϵ) was calculated assuming 100% current efficiency and conversion to gas bubbles, and that bubbles are uniformly distributed throughout the channel. For the case of $Re = 20$ and gas current of 120 mA, the total volume of hydrogen and oxygen gas produced is

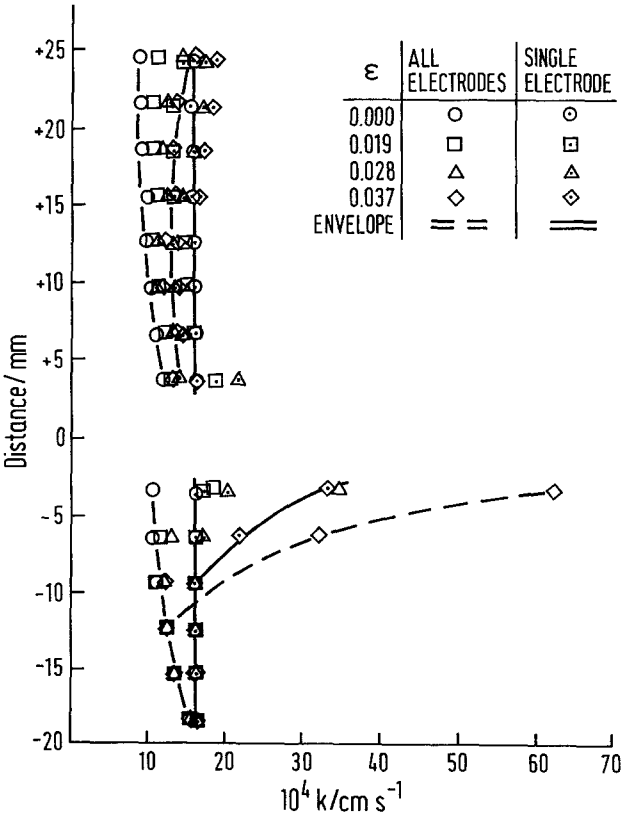

Fig. 5. Variation of mass transfer coefficient with distance from gas generating sites and gas void fraction at $Re = 20$.

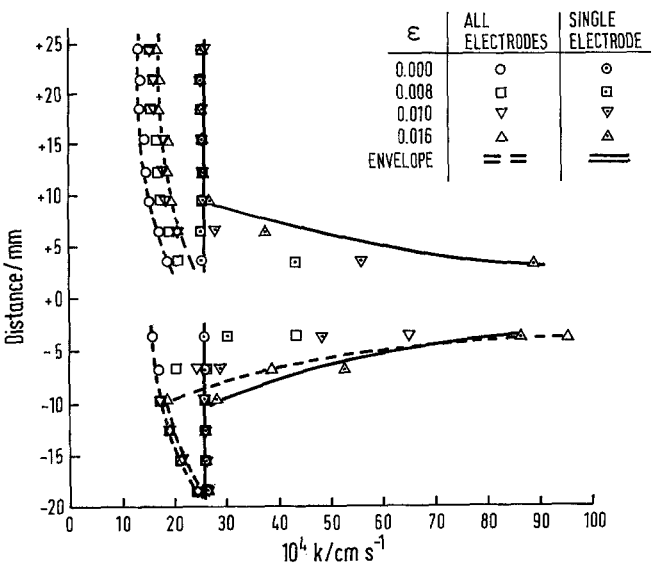

Fig. 6. Variation of mass transfer coefficient with distance from gas generating sites and gas void fraction at $Re = 70$.

$0.0212\,cm^3\,s^{-1}$. The volumetric flow rate of the electrolyte corresponding to $Re = 20$ is $0.57\,cm^3\,s^{-1}$. Hence, the estimated gas void fraction is 0.037.

The underlying assumptions in the above estimation are unlikely to be valid. A number of researchers [22–24] have proposed that practically all electrolytic gas generation is less than 100% efficient, that ϵ is substantially smaller than unity and that the true ϵ is very system dependent. Bubbles were observed mainly near the wall, and not in the middle of the channel, in the present experiments. Therefore, the calculated ϵ's in this work are estimates. Nonetheless, the estimated ϵ within the reactor was less than 0.05, and was well within the characterized bubble flow regime for two-phase flow in a chemical reactor.

As in the previous section, results in Figs 5 to 7 are discussed with reference to three regions: upstream electrodes, electrodes close to gas generation and downstream electrodes. At upstream electrodes far away from gas generation sites, k is practically independent of ϵ. And k varies marginally with distance in the case of all electrodes on, while it remains unaffected in the case of a single electrode on. Similar behaviour is evident at downstream electrodes away from gas generation sites. The only difference is in the case of all electrodes on, when k appears to depend to some extent on ϵ. As before, a larger k is generally observed in the case of a single electrode on compared to that in the case of all electrodes on. This, as remarked earlier, is due to the development of the concentration boundary layer in the latter case.

The marginal effect of ϵ on k is not unexpected in the presence of forced flow. The terminal velocity of 50 μm (typical bubble size in this study) bubbles can be estimated to be $\sim 2\,mm\,s^{-1}$ in stationary liquid compared with the liquid bulk velocity of $5.2\,mm\,s^{-1}$ at $Re = 20$.

In the vicinity of gas-generating microelectrodes, some interesting phenomena appear to occur in the presence of forced convection (Figs 5–7). At the first few upstream electrodes close to the microelectrodes, k increases significantly with ϵ in all six situations studied (i.e. three Re, all or one electrode on). The increase is as much as five times, depending on ϵ and the distance of the working electrodes from gas generation sites.

When all electrodes are on, k at all downstream electrodes exhibits similar marginal variation with ϵ irrespective of distance involved. But, in the case of a single electrode on, k at the first few downstream electrodes increases significantly with ϵ. And, k at distant downstream electrodes is practically unaffected by ϵ, except possibly at low Re (see Figs 5–7).

The enhancement in k due to gas bubbles is greatest in the immediate vicinity of gas generation sites. Hence, the percentage increase in k at the first working electrode on either side of gas-generating

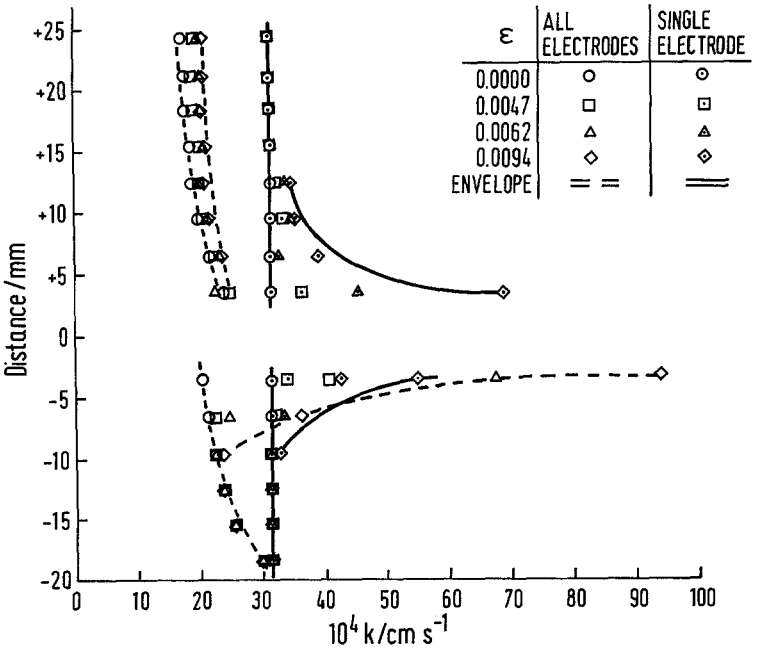

Fig. 7. Variation of mass transfer coefficient with distance from gas generating sites and gas void fraction at $Re = 120$.

Table 3. Effect of gas bubbles on k near gas generation sites in the presence of forced convection

(a) Re = 20

All or single electrode on	*Electrode position and number*	*Percentage increase in k for different ϵ*				*m**
		0.009	*0.019*	*0.028*	*0.037*	
All	d1	11	17	15	†	–
All	u1	4	76	280	490	3.54
Single	d1	12	15	35	†	–
Single	u1	3	6	25	105	2.47

(b) Re = 70

All or single electrode on	*Electrode position and number*	*Percentage increase in k for different ϵ*				*m**
		0.005	*0.008*	*0.010*	*0.016*	
All	d1	13	15	†	†	–
All	u1	53	169	302	494	2.02
Single	d1	25	70	120	250	2.07
Single	u1	4	20	90	240	3.81

(c) Re = 120

All or single electrode on	*Electrode position and number*	*Percentage increase in k for different ϵ*				*m**
		0.0031	*0.0047*	*0.0062*	*0.0094*	
All	d1	6	2	−5	†	–
All	u1	10	100	229	358	3.15
Single	d1	6	16	45	119	2.68
Single	u1	2	9	35	75	3.28

*Exponent in the correlation of percentage increase in k with ϵ^m.
†k could not be measured due to large fluctuations in i_L.

microelectrodes, is summarized in Table 3. The percentage increase was correlated with ϵ^m, and values of m thus obtained are also included in Table 3. (Correlation was not done when the enhancement was marginal and/or only a few data points were available.) The value of m is in the range 2 to 4, indicating significant increase in k with ϵ.

The marked contrast in the behaviour of the downstream electrodes (near the gas generation sites) between all electrodes on and one electrode on, is another surprising result. The only difference between these two modes is the developed boundary layer in the former operation. In the case of the single electrode on mode, the concentration boundary layer develops from the leading edge of that electrode only. The increase in k is generally greater at downstream than at upstream electrodes in the vicinity of gas generation. When all electrodes are on, there is a developed concentration boundary layer. And, in this situation, turbulent eddies near the wall due to gas generation are apparently less effective in enhancing mass transfer on the downstream side than on the upstream side.

The drastic increase in k with ϵ may be due to the interplay of a number of phenomena. When gas bubbles are present, many processes related to their formation, growth, detachment, upward travel, coalescence, and migration away from the wall region occur. These processes by themselves lead to improved mixing and, consequently, some increase in k at upstream electrodes close to gas generation sites, as suggested by the data in [7] and that in Fig. 4. The presence of forced convection superimposes liquid flow on the bubble processes thus leading to some complex interactions and the observed enhancement in k in Figs 5–7.

4. Conclusions

Experiments were conducted to measure mass transfer coefficient, k in a vertical parallel-plate electrochemical reactor with segmented copper electrodes as working electrodes and platinum microelectrodes for oxygen bubble generation. The range of conditions studied included: without and with gas bubbles; without and with liquid flow; and all or one

working electrode on mode. The estimated void fraction of gas, ϵ was less than 0.1 while *Re* was within 150. Results for k in some simple situations (namely, absence of gas bubbles and single electrode mode; presence of gas bubbles and quiescent electrolyte) are in accord with relevant correlations in the literature. These observations corroborate the validity of the present experimental procedures and data.

One of the main observations of this study was the drastic increase in k at both upstream and downstream working electrodes close to gas generation sites, with ϵ in the presence of forced flow. This may be due to the complex interplay of a number of processes related to gas bubbles and electrolyte flow. The results reported in this paper have shown the complexity of mass transfer enhancement by bubbles in a vertical parallel-plate cell. It follows that any application of experimental findings to industrial processes can only be made bearing in mind that the following factors affect the phenomenon: (a) position and manner of introduction of gas bubbles; (b) bubble size distribution and void fraction; (c) electrolyte flow and (d) size, position and operation mode of working electrodes, among others.

5. References

[1] R. E. W. Jansson and R. Marshall, *Electrochim. Act* **27** (1982) 823.
[2] W. S. Wu, G. P. Rangaiah and M. Fleischmann, *J. Appl. Electrochem.* **23** (1993) 113.
[3] H. Vogt, 'Gas Evolving Electrode in Comprehensive Treatise of Electrochemistry', Vol. 6 (edited by E. Yeager, J. O'M. Bockris, B. E. Conway and S. Sarangapani), Plenum Press, New York (1983).
[4] G. H. Sedahmed, *J. Appl. Electrochem.* **10** (1980) 351.
[5] A. M. Ahmed and G. H. Sedahmed, *J. Electrochem. Soc.* **135** (1988) 2766.
[6] H. Vogt, *Electrochim. Acta* **23** (1978) 203.
[7] C. I. Elsner and S. L. Marchiano, *J. Appl. Electrochem.* **12** (1982) 735.
[8] L. J. J. Janssen *ibid.* **17** (1987) 1177.
[9] H. Vogt, *ibid.* **19** (1989) 713.
[10] M. G. Fouad and G. H. Sedahmed, *Electrochim. Acta* **18** (1973) 55.
[11] L. J. J. Janssen and E. Barendrecht, *ibid.* **24** (1979) 693.
[12] M. F. Sherbiny, A. A. Zatout, M. Hussien, G. H. Sedahmed, *J. Appl. Electrochem.* **21** (1991) 537.
[13] P. J. Sides, 'Modern Aspects of Electrochemistry', No. 18 (edited by R. E. White), Plenum Press, New York (1986) 303.
[14] N. Ibl, *Electrochim. Acta* **24** (1979) 1105.
[15] L. Sigrist, O. Dossenbach and N. Ibl, *Int. J. Heat & Mass Transfer* **22** (1979) 1393.
[16] O. N. Cavatorta, U. Böhm and A. M. Chiappori De Del Giorgio, *J. Appl. Electrochem.* **21** (1991) 40.
[17] F. Giron, G. Valentin, M. Lebouche and A. Storck, *J. Appl. Electrochem.* **15** (1985) 557.
[18] C. W. Tobias, M. Eisenberg and C. R. Wilke, *J. Electrochem. Soc.* **99** (12) (1952) 359C.
[19] G. Marrucci and L. Nicodemo, *Chem. Engg. Sci.* **22** (1967) 1257.
[20] R. A. M. Al-Hayes and R. H. S. Winterton. *Int. J. Heat & Mass Transfer* **24** (1981) 223.
[21] D. J. Pickett, 'Electrochemical Reactor Design', Elsevier, Barking, UK (1977) Chapter 4.
[22] N. P. Brandon and G. H. Kelsall, *J. Appl. Electrochem.* **15** (1985) 475.
[23] G. Kreysa and M. Kuhn, *ibid.* **15** (1985) 517.
[24] H. Vogt, *ibid.* **17** (1987) 419.
[25] E. J. Fenech and C. W. Tobias, *Electrochim. Acta* **2** (1960) 311.